Renewable Energy 195 (2022) 1202–1217

Contents lists available at ScienceDirect

Renewable Energy

journal homepage: www.elsevier.com/locate/renene

# Technical-environmental-economic evaluation of biomass-based hybrid power system with energy storage for rural electrification

Alpaslan Demirci [a, *], Onur Akar [b], Zafer Ozturk [c]

[a] Department of Electrical Engineering, Yildiz Technical University, İstanbul, Turkey
[b] Department of Electronics and Automation, Marmara University, İstanbul, Turkey
[c] Department of Electrical and Electronic Engineering, Düzce University, Düzce, Turkey

ARTICLE INFO

*Article history:*
Received 10 November 2021
Received in revised form
14 June 2022
Accepted 18 June 2022
Available online 23 June 2022

*Keywords:*
Anaerobic digestion
Animal waste
Biomass
$CO_2$ emission
Hybrid power system
Industrial livestock farms

ABSTRACT

In recent years, higher penetrations of renewable energy generations helped persuade sustainable energy and environmental targets, although their intermittent and fluctuated nature raised technical challenges. However, hybrid power system can minimize these technical issues by integrating flexible generation capable renewable energy sources like biomass. This study deals with optimizing grid-integrated and stand-alone biomass-based hybrid power system for the energy demand of a rural region containing poultry farms. Besides solar and wind energy, energy storage integration is evaluated regarding overall technical-environmental-economic performance, considering the actual manure potential using HOMER Pro. In addition, sensitivity analyses are performed, considering the estimated load and inflations using an artificial neural network method. Using biomass and solar hybrid options offers more autonomous, environmentally friendly, and economic advantages. Biomass-based hybrid power system with solar energy reduced net present cost by around 12% and increased renewable fraction by 7%, and grid-connected options can provide 88.9% renewable fraction. In addition, the energy storage integration increased renewable fraction by around 10% and reduced excess energy by 16%. The proposed biomass-based hybrid power system achieves cost-effective sizing of solar or wind-based hybrid systems, empowers the reliability of renewable energy and presents good consistency of decarbonization targets.



## 1. Introduction

In the globalizing world, the increasing energy demand due to the growing population and developing industrialization is met mostly by fossil resources emitting greenhouse gases such as carbon dioxide ($CO_2$), methane ($CH_4$), and nitrous oxide ($N_2O$) [1]. The Paris Climate Agreement (2015) has been adopted worldwide to solve global warming and climate change by using renewable energy sources (RES) [2]. Therefore, biomass generation is expected to promising share in the energy supply in the future like the other RES such as solar, wind, geothermal, and hydro power. Bioenergy generation is becoming widespread because access to biomass can be planned and stored. The most common biomass sources are agricultural product waste, animal manure, food residues, aquatic plants and algae, and municipal solid waste. Industrial, animal, and vegetable waste increased due to consumption-society are also important greenhouse gas causes [3]. Methane gas emitted from animal waste is about 20 times more harmful than the same volume of $CO_2$. While the agriculture sector is responsible for 91%, 8%, and 5% of $NH_3$, $NO_x$, and $CH_4$ emissions, respectively, in Europe, 75% of $NH_3$ comes from livestock activities [4]. Animal manure contains high amounts of inorganic minerals and pathogens that have the potential to contaminate both soil and water sources. After heat treatment, these wastes must be disposed of to minimize bad odors and damage to nature and living things [5]. Biogas generally consists of 60% methane and approximately 40% carbon dioxide as an environmentally compatible energy source [6]. An anaerobic digestion (AD) is a biological process that produces biogas by breaking down organic compounds into simple substances by microorganisms in an oxygen-free environment [7,8]. Using biogas instead of natural gas, biochar instead of coal, and biodiesel instead of diesel helps to reduce greenhouse gases, odor, microbial pathogens, and produce organic fertilizers and carbon-neutral biofuels [9].

* Corresponding author.
*E-mail address:* ademirci@yildiz.edu.tr (A. Demirci).

https://doi.org/10.1016/j.renene.2022.06.097
0960-1481/

The worldwide biogas installed power has enlarged by around 90% between 2010 and 2018 (18.1 GW in 2018, compared to 8.2 GW in 2009), and further growth is expected. Europe contributed to the worldwide biogas generation with 64 TWH and North America with 15 TWH. Asia, Eurasia, South America, and Africa produced 4 TWh, 1.7 TWh, 953 GWh, and 89 GWh, respectively. The number of biogas plants in Europe reached 18,202 at the end of 2018. The leading country in the number of biogas plants was Germany (11,084 plants). Other leading countries are Italy (1655 facilities), France (837 facilities), the United Kingdom (715 facilities), and Switzerland (634 facilities), respectively [10]. Most biogas plants in Germany generate energy from energy crops (48.9%) and animal manure (44.5%) [11]. Germany's total electricity and heat production from biogas is approximately 33 TWh/year and 18.8 TWh/year, respectively. In addition, 97% of the fermentation residues are used in agriculture, and the rest is used for landscaping and other purposes [12–14]. The annual energy demand of Turkey is more than 300 TWh. Considering the country's population growth and economic expansion trends, whose energy demand has increased by 5% on average in the last two decades, annual energy demand is expected to increase by 3–4% over the next two decades. Turkey meets approximately 70% of its total energy needs from imported sources, and it is expected to increase to 90% in the following years. Although Turkey has a large lignite reserve, its economic benefits remain limited due to its low calorific value. Almost possible hydroelectric power plants have been installed, but their capacities will be insufficient for the increasing energy demand. Moreover, Turkey's high geothermal potential will not be able to respond to existing and future energy demand [15]. Therefore, renewable energy sources such as solar, wind and biomass are promising. While wind and solar energy generation share in 2019 is approximately 10%, the share of bioenergy remained at 1% [16]. The total recoverable bioenergy potential amount in Turkey is around 30 million tons and the average recycling rate is approximately 33%. Moreover, it is estimated to produce 52.5 MTOE of energy with biomass by 2030 [17]. However, inappropriate designs, incorrect maintenance-repair, lack of technical knowledge, incorrect planning, and seasonal raw material deficiencies are important barriers to biogas plants [18]. In addition, the trend of removing biomass from renewable energy incentives is likely to slow down the pace of new power plant investments due to regional political and economic uncertainties [19].

The recent studies on the increasing RES penetration and empowering rural electrification using biomass energy have been reviewed in terms of economics and environmental benefits [20]. An HPS offers stand-alone and grid-connected opportunities to access electricity in rural areas [21–24]. The basic principle of HPS is providing system control using different RES while minimizing installation costs [25]. The most suitable HPS is recommended for regions comparing the cost values related to environment, constraints, and targets [26]. A lower cost of energy (COE) than the grid electricity price has been achieved in the proposed HPS consisting of photovoltaic (PV) panels, wind turbines (WT), and biogas using HOMER Pro [27,28]. The energy generation feasibility of poultry waste in Pakistan has been reviewed considering the technological developments in the biogas industry and the energy generation predictions [29]. It has been proven that using poultry waste and rice husk effectively increases efficiency and environmental-friendly [7,30]. Another study was conducted on the energy savings potentials of unused meat waste for reducing fossil fuel dependences [31]. Off-grid HPS with PV-WT-BG for a village were optimized with HOMER, investigating technical and economic feasibility [32]. HPS with PV-WT-BG was proposed by integrating an energy storage system (ESS) [33]. Additionally, a case study on collecting biomass was conducted in India [34]. The performance of the proposed on-grid HPS with PV-BG for a village was compared to off-grid, and on-grid HPS has been offered as a cost-effective and reliable choice for rural electrification [35]. HPS with BG-DG-PV-ESS optimized and verified with HOMER for a hospital load in Saudi Arabia could reduce $CO_2$ emission and diesel consumption by approximately 84% and 81%, respectively [36]. Proposed HPS with PV-WT-BG-ESS can supply the peak demand during low renewable generation. It is also observed that the demand is supplied sufficiently, considering SOC of ESS and residual energy [37]. HPS with PV-WT-BG-DG was optimized using HOMER consisting of some fuel combinations. BG and other fuels have significantly reduced $CO_2$ emissions and doubled COE. On the other hand, much $CO_2$ is emitted if natural gas is used [38]. The smart eco-villages model of BG-PV offered for tropical countries like Malaysia can popularize RES [39]. HPS with PV-BG was proposed to power reliably and effectively agricultural wells in Iran. Optimization has shown that HPS with PV-BG gives better technical and economic results than HPS with only PV or BG [40]. Numerous studies have analyzed the technical and economic outcomes of HPS with PV-WT-BG using plant and animal wastes [41–50]. However, fewer studies have investigated poultry biogas electricity generation. Moreover, several studies have analyzed the gasification of poultry wastes [51,52]. However, most optimization studies on HPS with BG do not consider the grid constraints, energy sales prices, and changes in capital cost (CC) values. The original contributions of this study are as follows:

- The effects of using biomass as the energy source in industrial livestock farms and hybrid options with renewable energy sources are examined.
- The flexibility of biomass energy generation has been unlocked by optimizing HPS combinations.
- Energy storage has revealed the technical and economic potential if integrated into off-grid cases.
- Biomass integration can optimize the total cost of the hybrid system by reducing solar panel or wind turbine size.
- The reliability of solar and wind energy has been increased using biomass-based HPS and reduced fossil fuel usage.
- The environmental analysis determines the quantities of $CO_2$ emissions for twenty-five scenarios.
- The proposed grid-connected HPS options can provide 88.9% of the required power for the region.
- The multi-year investigations have considered the changes in the inflation rate and loads during the project's lifespan.

## 2. Material and methods

### 2.1. Load profile

This study was carried out located a region where poultry farms are concentrated in Reşadiye, Sakarya province in the Marmara region, at the coordinates of 40°36′4″ N, 30°40′37″ E. There are 1, 2, and 2 poultry farms having 40, 20, and 10 thousand poultries, respectively, and 150 houses. The daily energy consumption of poultry farms was approximated using the daily energy consumption measurement we made in 20 thousand chicken farms and last year's electricity bills. As a result, approximately 2225 kWh daily energy and 230.6 kW peak load were predicted for 5 poultry farms. The energy demand of 150 households is assumptions at approximately 732 kWh per day and a peak load of 110 kW. On the other hand, the socio-economic dynamics of the region create daily, monthly and seasonal differences in the electricity consumption pattern. For this reason, hourly and daily changes in electrical loads are assumed to be 20% and 10%, respectively. The location of the

region is seen in Fig. 1.

### 2.2. Photovoltaic

The regional average solar radiation was calculated as 3.96 kWh/m$^2$/day. Fig. 2 shows the region's GHI data. In synthesis, data is created using certain statistical features that reflect overall means.

The annual average solar radiation was calculated as 3.96 kWh/m$^2$/day, which the region is suitable for PV installation. The power output of a PV array is calculated as in Equation (1) [53]. Using the monthly average global solar radiation and the latitude of the site, HOMER uses an algorithm developed to generate hourly global solar radiation on horizontal surface data. This model considers the global solar radiation on a horizontal surface, the orientation of the PV, the location of the site on the Earth's surface, the time of year, and the time of day [54]. If the effect of temperature on PV array performance is neglected, then α can be assumed to be zero. The efficiency of the PV array is calculated by Equation (2) [55].

$$P_{PV}(t)=\begin{cases} Y_{PV}(t)\cdot f_{PV}\cdot\dfrac{G_T}{G_{T,stc}}\cdot\left(1+\alpha\cdot\left(T_C-T_{C,stc}\right)\right), & T_C\neq T_{C,stc} \\ Y_{PV}(t)\cdot f_{PV}\cdot\dfrac{G_T}{G_{T,stc}}, & \alpha=0 \end{cases} \tag{1}$$

$$\eta_{stc}=\frac{Y_{PV}}{A_{PV}\cdot G_{T,stc}} \tag{2}$$

Where $P_{PV}(t)$ is power output of a PV array (kW), $Y_{PV}(t)$ is the rated capacity of the PV array on the power output (under standart test conditions (STC)) (kW), $f_{PV}$ is PV derating factor (%), $G_T$ is the solar radiation incident on the PV array (kW/m$^2$), $G_{T,stc}$ is the incident radiation at STC (1 kW/m$^2$), $\alpha$ is the temperature coefficient of power ($-3.7\times10^{-3}$ 1/$^0$C), $T_C$ is the PV cell temperature ($^0$C), $T_{C,stc}$ is PV cell temperature under STC (25 °C) and $t$ is time (hour). Where $\eta_{stc}$ is the efficiency of the PV array (derating factor) (%) and $A_{PV}$ is surface area of PV array (m$^2$).

### 2.3. Wind turbine

The Weibull value is a measurement of the distribution of wind speeds throughout the year. The dependency factor is a measure of the randomness of the wind. Higher r1 values indicate that the hourly variation of wind speed is directly dependent on the wind speed in the previous hour, while lower values indicate that the wind speed tends to change randomly from hour to hour [1]. Fig. 3 shows the average wind speeds of the region. In this study, k = 2 and r1 = 0.85 were taken. The daily variation factor measures how much the wind speed depends on the hours of the day. In this study, 0.25 was taken. The hour of peak wind speed is the windiest hour of the day relative to the annual average. Anemometer height is taken as 10 m in HOMER simulations. The annual average wind data of the region has been determined as 3.78 m/s accordingly, the region is suitable for the establishment of low-powered wind turbines.

**Fig. 1.** The satellite view of Reşadiye.

The power output of a wind turbine is calculated as in Equation (3), and the wind speed acting on the wind turbine is calculated as in Equation (4) [56]. Where $P_{WT}(t)$ is output energy of a WT at the time (t) (kW), $P_r$ is rated power of WT (kW), $v_r$ is wind speed at WT height (m/s), $v(t)$ is the rated wind velocity (m/s), $v_{cin}$ is cut-in wind velocity of selected WT (m/s) and $v_{cout}$ is cut-off wind velocity of selected WT (m/s). Where $v_{anem}$ is wind speed at anemometer height (m/s), $v_r$ is wind speed at WT height (m/s), $Z_{anem}$ is anemometer height (10 m), $Z_{hub}$ is WT hub height (30 m) and λ is power coefficient (70–90%).

$$P_{WT}(t)=\begin{cases} 0 & v_{cin}\geq v(t)\ or\ v_{cout}\leq v(t) \\ P_r\dfrac{v(t)-v_{cin}}{v_r-v_{cout}} & v_{cin}\leq v(t)\leq v_r \\ P_r & v_r\leq v(t)\leq v_{cout} \end{cases} \tag{3}$$

$$v_r=v_{anem}\left(\frac{z_{hub}}{z_{anem}}\right)^{\lambda} \tag{4}$$

### 2.4. Biomass potential

The socio-economic benefits of biomass have always made it an important energy source for any country. In some countries, chicken manure is evaluated in many ways. Worldwide, 95% of chicken manure is used as compost fertilizer, cattle feed, and fuel. Animal manure is used to produce biogas due to Turkey's enormous requests for energy [8]. In rural areas of Turkey, the livestock sector is an essential source of employment for marginal and especially landless farmers. AD is the most popular energy conversion technique among all efficient energy conversion techniques. The AD process deals with the degradation of dung or any other organic matter by microbial movement, transforming it into biogas under anaerobic conditions [57]. This system collects the dung, already rich in microbes and mixed it with the required water to form a slurry. The recovered biogas from this process is later combusted in a combustion engine to generate electricity. One poultry produces an average of 0.08–0.1 kg of wet manure per day [58]. Therefore, between 40 and 78 m$^3$ of biogas can be produced with 1 ton of wet chicken manure. The amount of heat provided by 1 m$^3$ of biogas is 4700–5700 kCal. This value is equivalent to the energy provided by 0.66 L of diesel, 0.75 L of gasoline, and 0.25 m$^3$ of propane. The generated biogas has a composition of methane (60–70%), carbon dioxide (30–40%), hydrogen sulfide, and ammonia (traces) and has a calorific value of 16–25 MJ/m$^3$ and the electrical energy content of biogas is 4.5–7 kWh/m$^3$ of biogas [12,59]. Fig. 4 shows the energy production stages with biogas from raw material to final use.

$$M_{daily}^{total}=M_{daily}^{wet}\cdot T_S \tag{5}$$

$$B_A=0,365\cdot P_{livestock}\cdot M_{daily}^{total}\cdot C_b \tag{6}$$

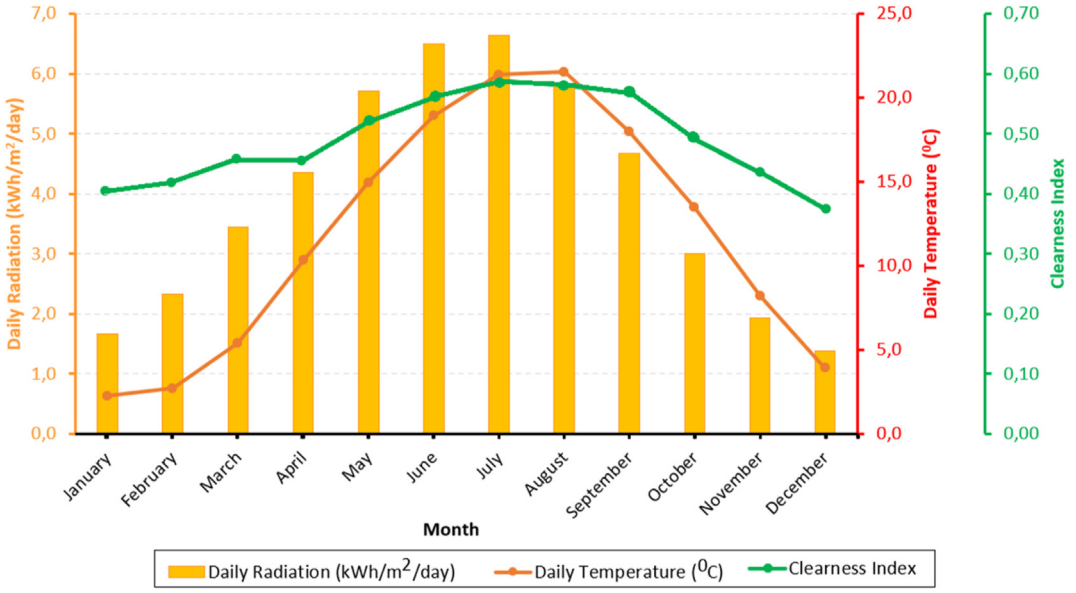


**Fig. 2.** The average weather condition for the region.

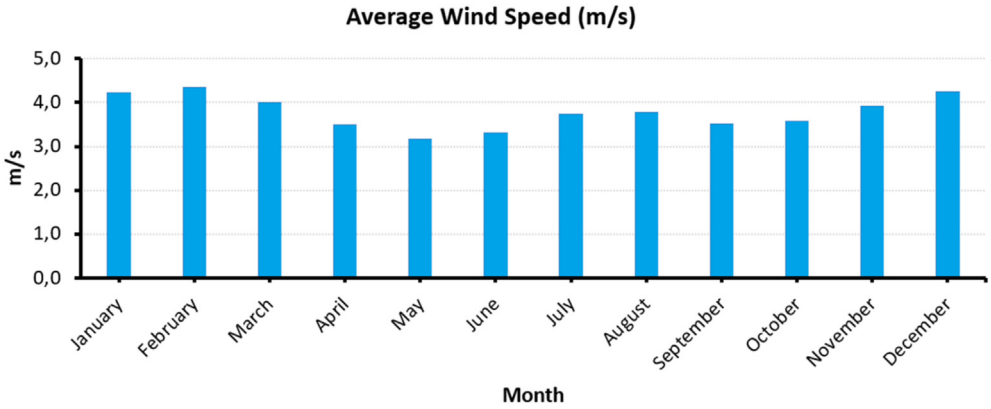


**Fig. 3.** The average wind speed in Reşadiye.


**Fig. 4.** Bio-power from feedstock to end-use.

$$B_T = B_A \ . C_C \quad (7)$$

$$B_E = B_A \ . C_E \quad (8)$$

Where the daily collectible manure amount is given in Equation (5), biogas amount is given in Equation (6), caloric biogas value is given in Equation (7), and biogas-based electrical energy is given in Equation (8) [60]. Where the daily amount of manure per animal (kg. day/number) is $M_{daily}^{total}$, daily raw manure (kg.day/number) is $M_{daily}^{wet}$, the period of stay in the shelter of animals (%) is $T_s$,biogas amount ($m^3$/year) is $B_A$, calorific energy of biogas (MJ) is $B_T$, livestock population is $P_{livestock}$, biogas coefficient ($m^3$/kg) is$C_b$, calorific biogas coefficient (MJ/$m^3$) is $C_c$, biogas electric energy (kWh) is $B_E$,and electric coefficient (%) is $C_E$. This study analyses daily poultry animal waste per head 0.1 kg/day, biogas coefficient 0.04 $m^3$/kg, methane content 60% with calorific value 21.5 MJ/$m^3$, electric energy coefficient 35% considering parameters. In addition, the amount of animal waste obtained according to the growing model varies, and the staying time of the meat poultry in the barn is 100% in this study.

### 2.5. Energy storage system (ESS)

Lead-acid batteries are the oldest and well-matured technology for storing electrical energy. Lead-acid batteries are used more frequently, serving as storage in many areas, thanks to the low investment cost, the lowest self-discharge among all rechargeable batteries, and relatively easy maintenance. [61]. The number of battery cell is given in Equation (9) [62]. Where $C_{BAT}$ is battery capacity (Ah), $C_{Wh}$ is battery pack (ESS) capacity (kWh) and $N_{ESS}$ is the number of battery cells.

$$N_{ESS} = \frac{C_{Wh}}{C_{BAT}} \tag{9}$$

### 2.6. Converter

Bidirectional power converters are used in hybrid power systems to maintain energy flow between direct current (DC) and alternating current (AC) buses. They have two functions: the rectifier (which converts DC into AC) and the inverter (which converts AC into DC) [38]. The inverter efficiency ($\eta_i$) is the ratio between the output power generated by the inverter and its input power, as shown in Equation (10).

$$\eta_i = \frac{P_{io}}{P_{ii}} \tag{10}$$

$$\eta_r = \frac{P_{ro}}{P_{ri}} \tag{11}$$

Where $P_{io}$ is the output power of the inverter (kW), and $P_{ii}$ is the input power of the inverter (kW). The rectifier efficiency ($\eta_r$) is the ratio between the output power generated by the rectifier and its input power, as shown in Equation (11). $P_{ro}$ is the output power of the inverter (kW), and $P_{ri}$ is the input power of the inverter (kW). Inverter and rectifier efficiency are considered 95%, and their useful life is up to 15 years [63].

### 2.7. Electrical load and inflation forecasting using artificial neural networks

In this section, the energy demand of the poultry farm and its nearby region is forecasted with artificial neural networks (ANN), one of the commonly used forecasting methods. Accurate load forecasting and planning reduce operating costs and losses, offering numerous technical and economic benefits for both the generator and the consumer [53]. The yearly poultry variations and other parameters are modeled with the ANN in Fig. 5.

The data set required for ANN includes load characteristics, population, total electricity consumption per capita, GDP, East Marmara GDP, DM poultry (chicken) number, inflation, net migration, unemployment rate, and electrical energy production between 2000 and 2020. It was formed by considering the annual population growth factors of Turkey and Sakarya. Equation (12) shows the resultant y function, and Equation (13) shows the ReLu activation function.

$$y = \sum_{i=1}^{n} f(x_i \,.\, W_i + b) \tag{12}$$

$$f(x) = \begin{cases} x & if\ x > 0 \\ 0 & if\ x \le 0 \end{cases} \quad [0,\ \infty) \tag{13}$$

Equation (12), y is the result, f is the activation function, w is the weight coefficient, x is the input values, and b is the threshold coefficient. Activation function features used in ANN applications have a high impact on training dynamics and task performance. In this study, the ReLU activation function, which is preferred especially in multi-layer networks due to its simplicity and low computational load in inflation and load estimation, is used in Equation (13). The weights in the created model neural networks are optimized using the Adam solver function. MSE and $R^2$ functions are used to calculate the error and success of the model. Performance function of MSE in Equation (14), $x_j$ represents the data list and $y_j$ shows the estimated values. $SS_{pred}$ in Equation (16) is the sum of the squares of the difference between the real values in the data set in Equation (15) and the estimated values by the model. $f_i$ is model output, $\bar{y}$ is the average of the observation values. $SS_{total}$ in Equation (17) is calculated by summing the squares of $\bar{y}$, which is the mean of all the observation values, and the difference from the $y_i$ is specified in the data set.

$$MSE(x, y) = \frac{1}{N}\sum_{i=1}^{n}\left(x_j - y_j\right)^2 \tag{14}$$

$$R^2 = 1 - \frac{SS_{pred}}{SS_{total}} \tag{15}$$

$$SS_{pred} = \sum_i (f_i - \bar{y})^2 \tag{16}$$

$$SS_{total} = \sum_i (y_i - \bar{y})^2 \tag{17}$$

Fig. 6 shows the inflation and energy demand forecasts for the years 2021–2040 obtained from the ANN training.

The success of the forecasts using ANN considering the data between 2000 and 2020 are given in Table 1. The results show that the developed forecast model can be used reliably.

### 2.8. Economic analysis

Net present cost includes installation and operating costs over the life of the system. Next, the economic outputs of the system are calculated to find the net present cost. Finally, the net present cost is calculated using Equation (18). Where *NPC* is net present cost ($), $C_{cap}$ is capital cost ($), $C_{rep}$ is replacement cost ($), $C_{O\&M}$ is operation and maintenance cost ($) and $C_{salvage}$ is salvage cost ($).

$$NPC = \frac{C_{ann,total}}{CRF(i,N)} = \frac{C_{cap} + C_{rep} + C_{O\&M} - C_{salvage}}{CRF(i,\ N)} \tag{18}$$

The capital recovery factor is used to calculate the present value of the annual income expense stream. It is calculated by Equation (19).

$$CRF(i,N) = \frac{i\,.\,(i+1)^N}{(i+1)^N - 1} \tag{19}$$

HOMER defines the unit energy cost as the average cost per kWh of the useful electrical energy produced by the system and explains it with Equation (20). Where *COE* is cost of energy ($/kWh), $C_{ann,tot}$ is total system annualised cost ($), $E_{prim}$ is primary energy sold to the utility grid (kWh), $E_{def}$ is deferrable energy sold to the utility grid (kWh), $E_{grid,sales}$ is electrical energy sold to the utility grid (kWh), *NPC* is net present cost ($), $CRF(i,\ N)$ is capital recovery factor (%), $i$ is annual real interest rate (%), $N$ is project time (year),

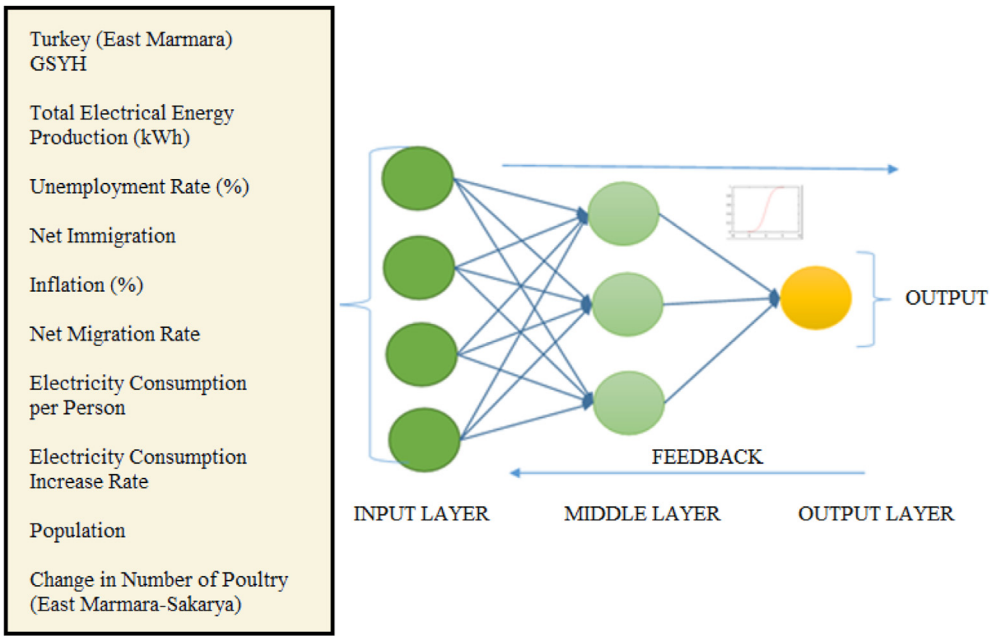


**Fig. 5.** Artificial neural network model.

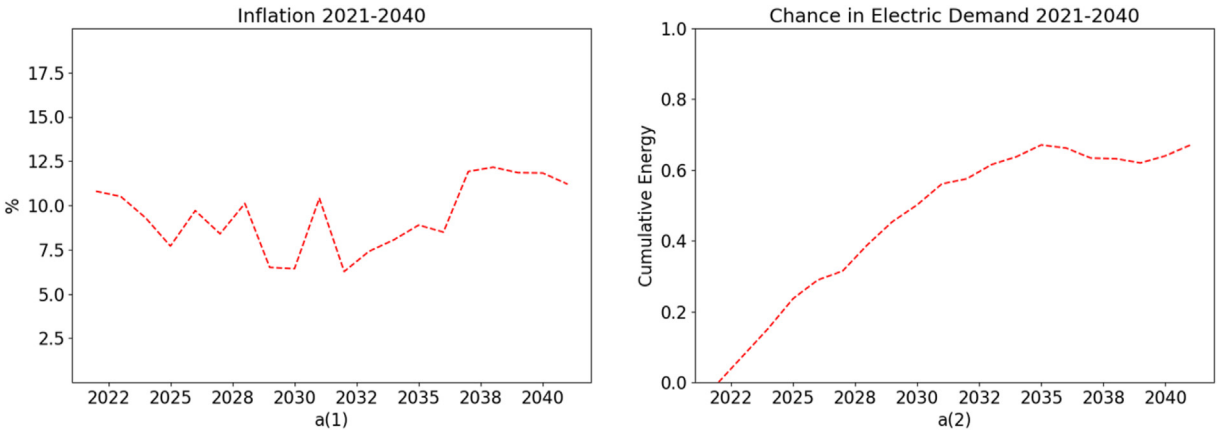


**Fig. 6.** The forecasts of inflation and energy demand for 2021–2040.

**Table 1**
The success of inflation and load demand forecasts using ANN.

| | Inflation Forecast | Energy Demand Forecast |
|---|---|---|
| **MSE** | 0.036 | 0.0014 |
| **$R^2$** | 0.989 | 0.9847 |

and $E_{gen}(t)$ is generates (PV) total energy in t hours (kWh) [64].

$$COE = \frac{C_{ann,tot}}{E_{prim} + E_{def} + E_{grid,sales}} = \frac{NPC \,.\, CRF(i,\ N)}{\sum_{t=0}^{t=N} E_{gen}(t)} \tag{20}$$

Residual power ($P_{residual}$) is obtained by subtracting the sum of demand ($P_{load}$) and loss ($P_{tot_{loss}}$) power from the installed RES power ($P_{RESgen}$), as expressed in Equation (21). The excessive power ($P_{EE}$), which cannot be used completely due to the limitations imposed on $P_{residual}$, is expressed in Equation (22). $c_{pv}^{limit}$ is the power limitation coefficient varying between 0 and 1 in Equation (23), and it has been taken within 0.4–0.6 in several studies. Accordingly, $c_{pv}^{limit}$ has been taken as 0.4 in the technical and economic analyzes of this study. The daily available biomass reserve is $S_{biomass}^{avability}$ as seen in Equation (24). $E_{BAT}(t)$ is the energy stored in each battery, $E_{BAT}^{max}$ and $E_{BAT}^{min}$, represents the maximum and minimum allowable amounts of energy for storage in each battery, respectively, in Equation (25).

$$P_{RE}(t) = P_{RES_{gen}}(t) - P_{load}(t) - P_{tot_{loss}}(t) \tag{21}$$

$$P_{EE}(t) = P_{RE}(t) - P_{PV_{nom}} . c_{pv}^{limit}\ ,\ \forall \in P_{RE}(t) > P_{PV_{nom}} . c_{pv}^{limit} \tag{22}$$

$$0 < c_{pv}^{limit} < 1 \tag{23}$$

$$S_{biomass_{\min}}^{avability} \leq S_{biomass}^{avability} \leq S_{biomass_{\max}}^{avability} \tag{24}$$

$$E_{BAT}^{min} < E_{BAT}(t) < E_{BAT}^{max} \tag{25}$$

Self-consumption rate and self-feeding rates have been common performance indicators in numerous studies in the literature. The SCR is defined in Equation (26) as the ratio between the BG energy transferred directly to the load and the annual total BG production. SSR is defined as the ratio between the total generation of BG transferred directly to the load and the annual total load demand. As seen in Equation (27), if the BG share in the load demand increases, the SSR increases.

$$SCR = \frac{\sum E_{BG}^{cons}}{\sum E_{BG}^{gen}} (\%) \quad (26)$$

$$SSR = \frac{\sum E_{BG}^{cons}}{\sum E_{Load}} (\%) \quad (27)$$

## 3. Simulation and results

Fig. 7 shows the HPS model flowchart. The micro HPS system was optimized by defining the ANN estimates, biomass reserves, and other components' costs.

### 3.1. HPS models

Three HPS models include on-grid and several off-grid scenarios shown in Fig. 8. The technical and economic parameters used in the system are shown in Table 2.

The grid energy sell price was determined as 0.08 $/kWh, grid energy buy price was 0.13 $/kWh, the inflation rate was 11%, DR was 6%, the diesel fuel cost was 1.1 $/L, project life was 20 years, and biomass average waste cost was 25 $/t [59,65].

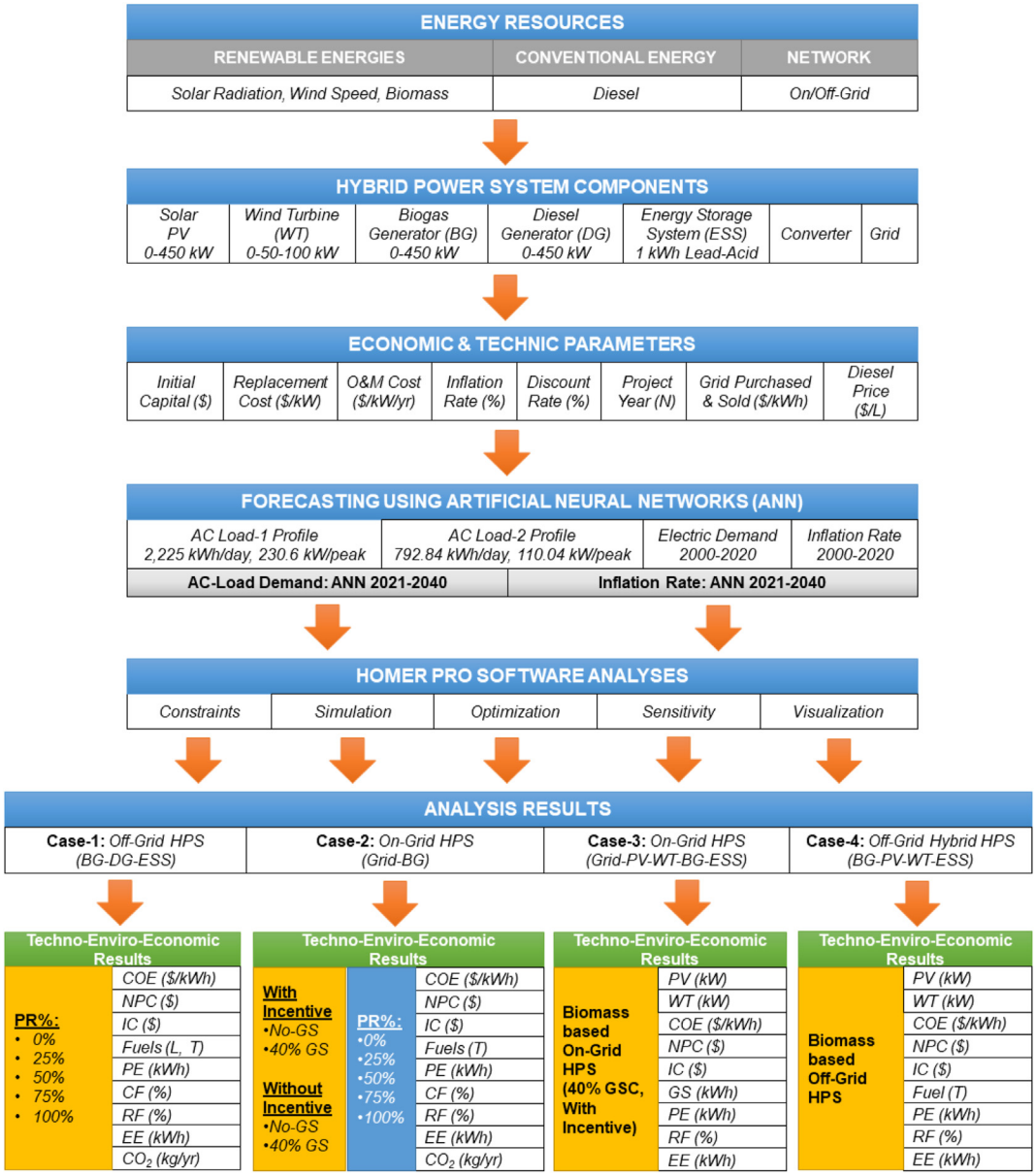


**Fig. 7.** The flow chart of HPS.

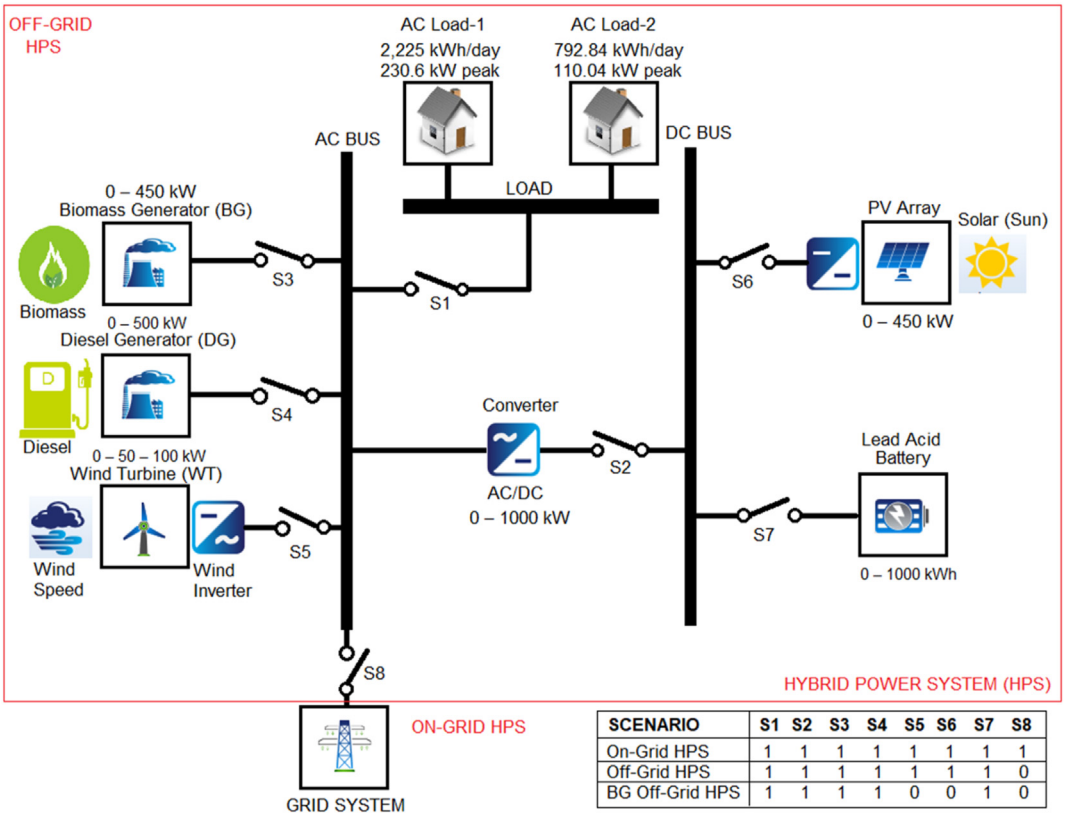


| SCENARIO | S1 | S2 | S3 | S4 | S5 | S6 | S7 | S8 |
|---|---|---|---|---|---|---|---|---|
| On-Grid HPS | 1 | 1 | 1 | 1 | 1 | 1 | 1 | 1 |
| Off-Grid HPS | 1 | 1 | 1 | 1 | 1 | 1 | 1 | 0 |
| BG Off-Grid HPS | 1 | 1 | 1 | 1 | 0 | 0 | 1 | 0 |

**Fig. 8.** On-grid and off-grid HPS models.

**Table 2**
Performance of forecasts using ANN.

| Design | Lifetime | Capital [$/kW] | Replacement [$/kW] | O&M |
|---|---|---|---|---|
| **BG** | 20,000 h | 1690 | 1300 | 0.0054 $/hour/kW |
| **DG** | 15,000 h | 500 | 500 | 0.05 $/hour/kW |
| **WT** | 20 year | 3185 | 2600 | 20 $/year/kW |
| **PV** | 20 year | 1000 | 900 | 20 $/year/kW |
| **Converter** | 20 year | 400 | 400 | 0.01 $/year/kW |
| **ESS** | 20 year | 225 $/kWh | 150 $/kWh | 10 $/year/kWh |

### 3.2. Optimization Results-1 (off-grid HPS with only BG-DG)

Table 3 shows the optimization results of off-grid HPS with only BG-DG, where PR changes are valid only for BG. The optimal NPC realized in 50% PR. CF has decreased non-linearly due to the large installed power dimensions for more than 50% PR. The optimum ESS size is reduced while PR is increased. However, there is an inevitable increase in EE due to increased PR. The $CO_2$ value seen in Fig. 9 is approximately the same value at more than 50% PRs, with the least emission at 75% PR. While RFs are 98% and above in 50% PR, RF is 59.2%, although CF is 90.7% in 25% PR.

### 3.3. Optimization results –2 (on-grid HPS with BG)

Table 4 shows the optimization results of on-grid HPS with only BG, where PR changes are valid only for BG.

In the case of WI and no-GSC, the optimal COE result was achieved at 75% PR. Although BG has high CF before 75% PR, the COE is greater than 29% compared to 75% PR because the BG size is not optimal. However, approximately 41% of GS could be met at 100% PR compared to 100% PR without GSC. Thus, CF reduced and slightly increased the NPC compared to 75% PR. In the case of WI, it was determined that despite the increase in BG dimensions, GSC

**Table 3**
Optimization Results-1 (off-grid HPS with BG-DG).

| BG PR (%) | DG (kW) | BG (KW) | ESS (kWh) | IC (M$) | NPC (M$) | COE ($/kWh) | Diesel (L) | Biomass (T) | PE (MWh/yr) | CF (%) | RF (%) | EE (kWh/yr) | $CO_2$ (kg/yr) |
|---|---|---|---|---|---|---|---|---|---|---|---|---|---|
| **-** | 400 | - | - | 0.20 | 19.7 | 0.513 | 370,884 | - | 1,295.6 | 37.0 | - | 147,589 | 971,910 |
| **25** | 400 | 90 | 1689 | 0.73 | 9.47 | 0.247 | 122,172 | 3821 | 764.0 | 90.7 | 59.2 | 9.08 | 334,522 |
| **50** | 400 | 180 | 1178 | 0.80 | 4.65 | 0.121 | 4589 | 5973 | 1,176.6 | 74.8 | 98.5 | 19,632 | 31,028 |
| **75** | 400 | 270 | 350 | 0.81 | 5.39 | 0.140 | 232 | 6268 | 1,213.9 | 51.4 | 99.9 | 36,951 | 20,695 |
| **100** | 400 | 360 | 432 | 0.98 | 6.71 | 0.175 | - | 6540 | 1,254.6 | 39.9 | 100 | 43,289 | 21,525 |

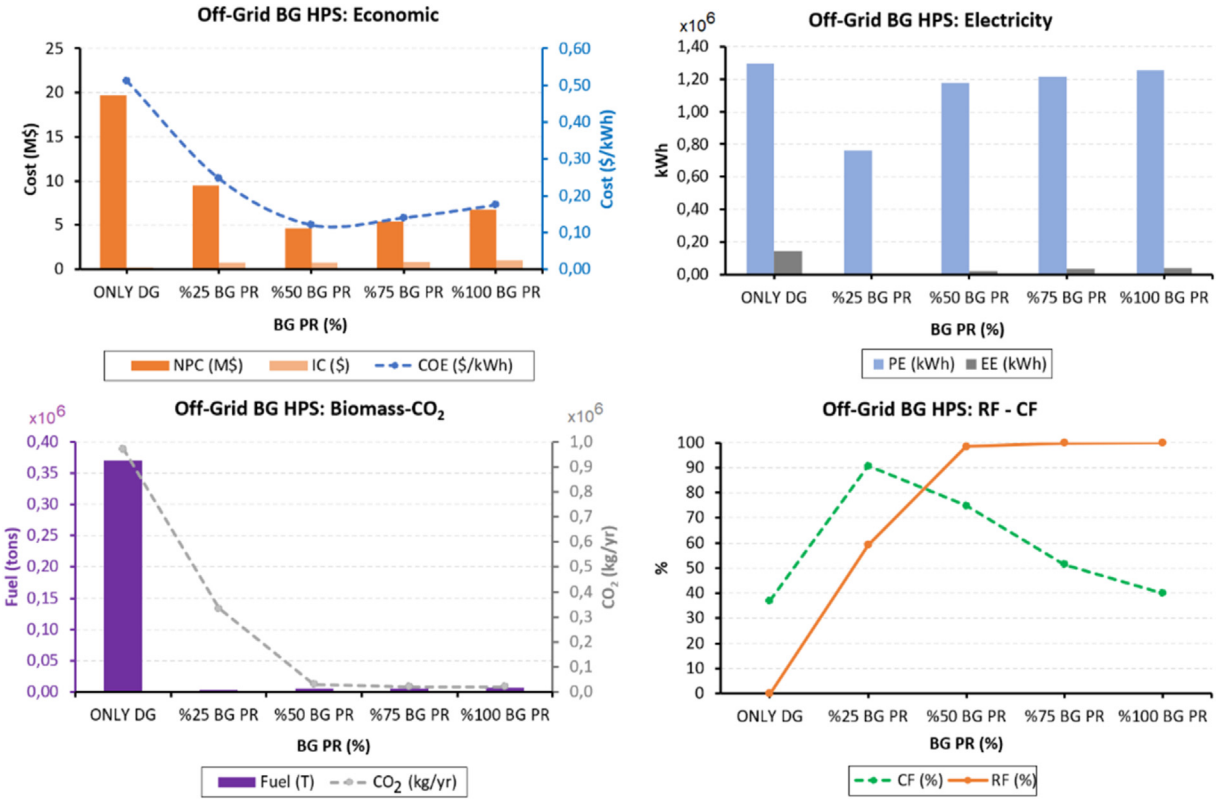


**Fig. 9.** Technical-economic variations in off-grid HPS with only BG-DG.

**Table 4**
Optimization results –2 (on-grid HPS with BG).

| BG PR (%) | Without incentive (WOI) (With %40 Grid sale constraint) | | | | | | | With incentive (WI) (With %40 Grid sale constraint) | | | | | | |
|---|---|---|---|---|---|---|---|---|---|---|---|---|---|---|
| | IC (M$) | NPC (M$) | COE ($/kWh) | GS (MWh/yr) | PE (MWh/yr) | CF (%) | $CO_2$ (kg/yr) | IC (M$) | NPC (M$) | COE ($/kWh) | GS (MWh/yr) | PE (MWh/yr) | CF (%) | $CO_2$ (kg/yr) |
| **-** | - | 3.07 | 0.080 | - | - | - | 727,482 | - | 3.07 | 0.080 | - | - | - | 727,482 |
| **25** | 0.15 | 3.04 | 0.079 | - | 287.3 | 36.5 | 550,304 | 0.15 | 2.96 | 0.074 | 37.6 | 502.1 | 63.4 | 443,276 |
| **50** | 0.30 | 3.01 | 0.078 | - | 212.9 | 13.8 | 593,101 | 0.30 | 2.51 | 0.048 | 383.9 | 1,343.4 | 85.4 | 140,809 |
| **75** | 0.45 | 2.81 | 0.073 | - | 21.1 | 0.900 | 714,344 | 0.46 | 2.30 | 0.037 | 682.0 | 1,719.3 | 72.9 | 95,939 |
| **100** | 0.61 | 2.71 | 0.070 | - | - | 0.0 | 727,482 | 0.61 | 2.33 | 0.037 | 704.2 | 1,541.1 | 49.1 | 218,466 |
| **BG PR (%)** | **Without incentive (WOI) (No Grid sale constraint)** | | | | | | | **With incentive (WI) (No Grid sale constraint)** | | | | | | |
| | **IC (M$)** | **NPC (M$)** | **COE ($/kWh)** | **GS (MWh/yr)** | **PE (MWh/yr)** | **CF (%)** | **$CO_2$ (kg/yr)** | **IC (M$)** | **NPC (M$)** | **COE ($/kWh)** | **GS (MWh/yr)** | **PE (MWh/yr)** | **CF (%)** | **$CO_2$ (kg/yr)** |
| **-** | - | 3.07 | 0.080 | - | - | - | 727,482 | - | 3.07 | 0.080 | - | - | - | 727,482 |
| **25** | 0.15 | 3.04 | 0.079 | - | 287.3 | 36.5 | 550,304 | 0.15 | 2.96 | 0.074 | 39.2 | 503.8 | 63.6 | 443,274 |
| **50** | 0.30 | 3.01 | 0.078 | - | 212.9 | 13.8 | 592,101 | 0.30 | 2.13 | 0.038 | 492.7 | 1,461.9 | 92.8 | 137,323 |
| **75** | 0.46 | 2.81 | 0.073 | - | 21.1 | 0.902 | 714,344 | 0.46 | 1.26 | 0.016 | 1,108.4 | 2,184.9 | 92.4 | 82,162 |
| **100** | 0.61 | 2.71 | 0.070 | - | - | 0.0 | 727,482 | 0.61 | 1.21 | 0.014 | 1,335.7 | 2,177.6 | 69.1 | 230,406 |

prevented the rise of PE and COE increased significantly compared to the scenarios without GSC. GS decreased by only 4% for WI GSC, and no- GSC and COE remained approximately the same at 25% PR, which refers to the lowest installed capacity. Although the RF in scenarios with WI were higher than 50% PR, the best COE was achieved in 75% PR. Due to high COE, CF of BGs decreased significantly in WOI scenarios, especially 0% in 75% and above PRs. In addition, although the BG had a 25% PR due to WOI, the highest RF value was realized in Fig. 11. As seen in Fig. 10, IC changes linearly depending on the PR. However, the COE did not change linearly due to GSCs with WI and WOI. The CF decreases in the case of GSC with WI, as seen in Table 5. Therefore, the COE increases compared to No-GSC with WI. In addition, the COE changed slightly in scenarios with WI, and the NPC remained nearly constant in 75% and above PR. A decrease in GS revenues in WOI scenarios hindered the improvement of COE and NPC. Therefore, it has been determined that the optimal scenarios are experienced, especially in 50–75% PR. However, CF is less than 50% in all scenarios with WOI, and power plant installations are not suitable in these scenarios.

Fig. 11 shows the RF, CF, PE, and GS values obtained as an optimization result of On-Grid HPS with BG. In the case of GSC in scenarios with WI, it was observed that RF did not change much at 25–50% PR. However, RF decreased significantly in both GS scenarios with WOI, especially 50% and above PR. Although RF was lower in 50% and below PR with WOI, RF was nearly the same in both No-GSC and GSC scenarios. In No-GSC scenarios with WI, CF

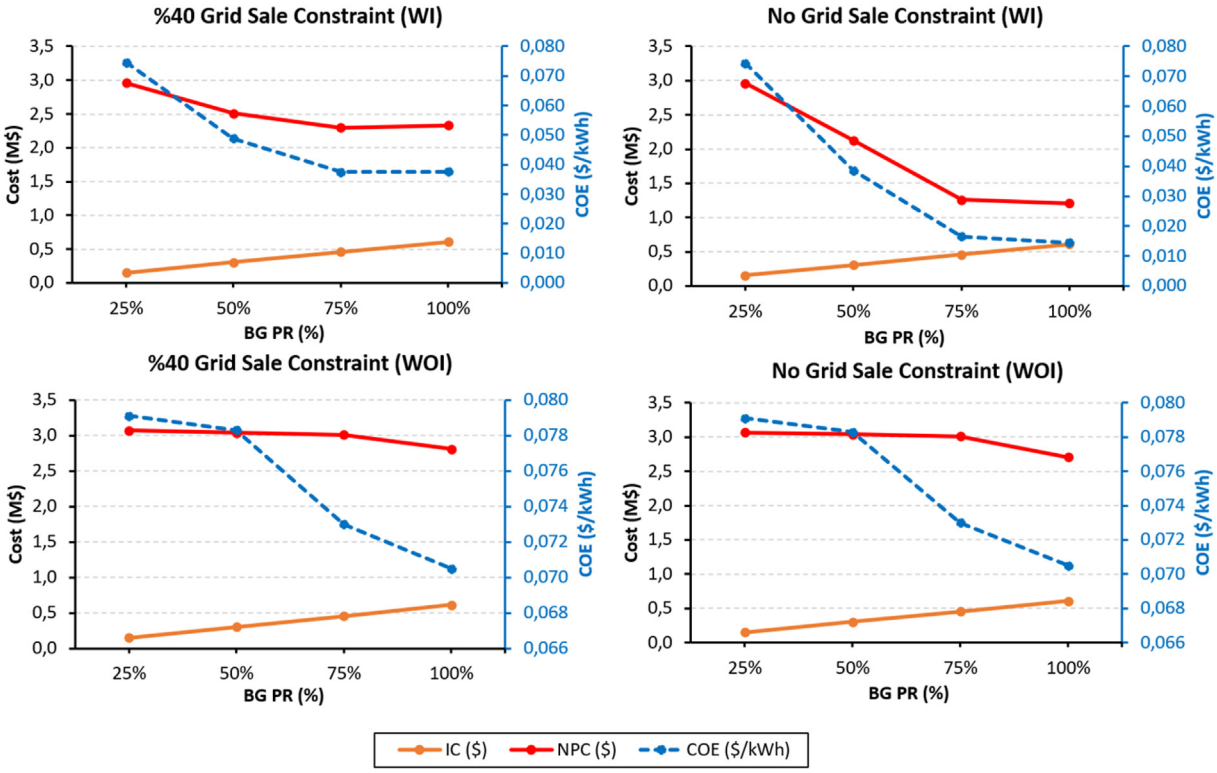


**Fig. 10.** The economic effects of incentives (WI-WOI) on On-Grid HPS with only BG.

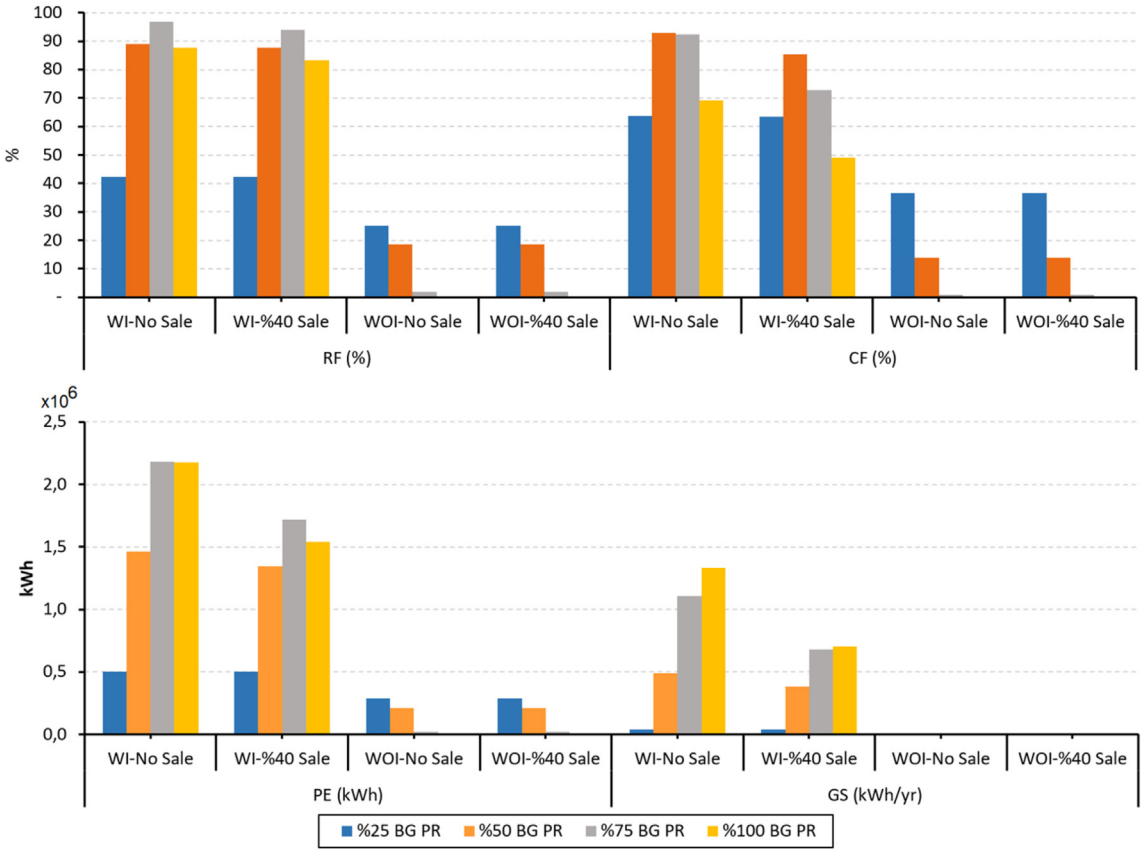


**Fig. 11.** The variations of energy generation and grid selling according to optimization of On-Grid HPS.

**Table 5**
The system performance of On-grid HPS RES with 100% PR.

| Case | BG (kW) | WT (kW) | PV (kW) | COE ($/kWh) | NPC (M$) | IC (M$) | PE (MWh/yr) | GS (MWh/yr) | RF (%) | EE (kWh/yr) |
|---|---|---|---|---|---|---|---|---|---|---|
| **M1** | **90** | - | 270 | 0.063 | 2.62 | 0.52 | 458.5 | 87.2 | 62.2 | 21,680 |
| **M2** | | 50 | 220 | 0.064 | 2.68 | 0.63 | 477.2 | 91.2 | 64.7 | 11,096 |
| **M3** | | 150 | 120 | 0.069 | 2.87 | 0.85 | 483.6 | 89.6 | 66.3 | 7286 |
| **M4** | | 250 | 20 | 0.074 | 3.10 | 1.07 | 470.1 | 92.4 | 64.7 | 21,414 |
| **M5** | **180** | - | 180 | 0.040 | 2.07 | 0.79 | 1,130.5 | 371.1 | 88.9 | 14.7 |
| **M6** | | 50 | 130 | 0.048 | 2.48 | 0.69 | 1,135.9 | 373.6 | 89.5 | 0 |
| **M7** | | 100 | 80 | 0.050 | 2.58 | 0.80 | 1,135.2 | 372.8 | 89.7 | 36.0 |
| **M8** | | 150 | 30 | 0.052 | 2.67 | 0.91 | 1,135.0 | 374.3 | 90.0 | 245 |
| **M9** | **270** | - | 90 | 0.040 | 2.35 | 0.65 | 1,496.7 | 609.1 | 91.5 | 0 |
| **M10** | | 50 | 40 | 0.046 | 2.71 | 1.19 | 1,483.5 | 608.0 | 91.1 | 0 |

takes approximately the same values up to 75% PR, but CF is reduced by 48% in the case of GSC in 100% PR. PE increases due to CF in scenarios with WI. In the case of GSC, the optimal results were obtained at 50–75% PR. It has been observed that GS occurs in GSC and No-GSC scenarios with WI, and No-GSC increases GS in parallel with CF, especially in the case with WI. It has been observed that GS has reduced by 50% in scenarios of No-GSC 50% and above PR.

Fig. 12 shows the IRR, DP, SCR, and SSR as optimization results of on-grid HPS. The IRR was as high as 10.10% and 14.50% at 50% and 100% PR with No-GSC, respectively. On the other hand, COE with WI took higher values in GSC than in No-GSC scenarios. At the same time, CF decreased, and IRR reduced by 50% approximately. Despite 25% PR with WI, DP did not occur, and IRR was 0% on both GS sales values. CF in GSC scenarios decreased, especially at 100% PR. Therefore, IRR decreased to 2% as IC and O&M could not be met with current production. DP was 10 years or less in both GSC and No-GSC scenarios for 50% and above PR with WI. DP in both GS took approximately 14 years for 25% PR with WI. However, DP has values close to the project life of 20 years in all PRs with WOI. SCR decreased with increasing BG size in PRs with WI. Both GS with WI had the highest SCR rate in 25% PR. However, SCR rates were 100% in all PRs with WOI due to the low GS price. However, bioenergy was not generated in 100% PR with WOI due to high COE. Thus, SCR and SSR were 0%. SSR is the same for PRs with WI in GSC and No-GSC scenarios, and BG has the optimal value of 75% PR. On the other hand, SSR in WOI took values less than realized in WI due to the decrease in GS revenues. Therefore, the SSR was 0% in 100% PR with WOI.

Fig. 13 shows the $CO_2$ emissions of both on-grid and off-grid. The lowest emission for both GSC and No-GSC is 75% PR with WI. $CO_2$ emission reduced by 16%, especially in No-GSC scenarios due to the increase in SSR. The rise in COE of WOI reduces SSR and increases $CO_2$ emissions, as it happens in only grid scenarios. $CO_2$ emissions are minimized due to the SSR in off-grid HPS approaching 100% for 50% and above PR. The $CO_2$ emission, especially in the case of 25% PR, is very high compared to other off-grid scenarios since the installed power cannot meet the load demand. The results show that optimal HPS sizing will reduce COE and minimize $CO_2$

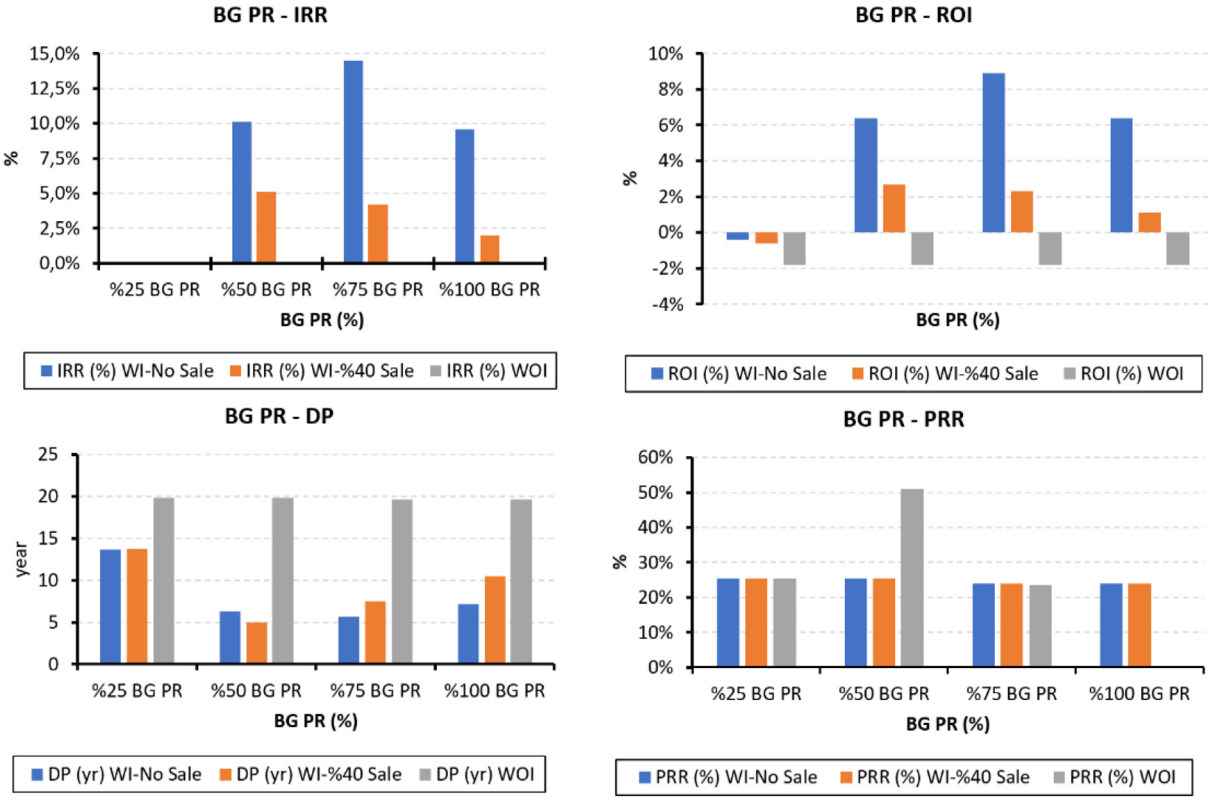


**Fig. 12.** Technical-economic indicators for WI and WOI cases.

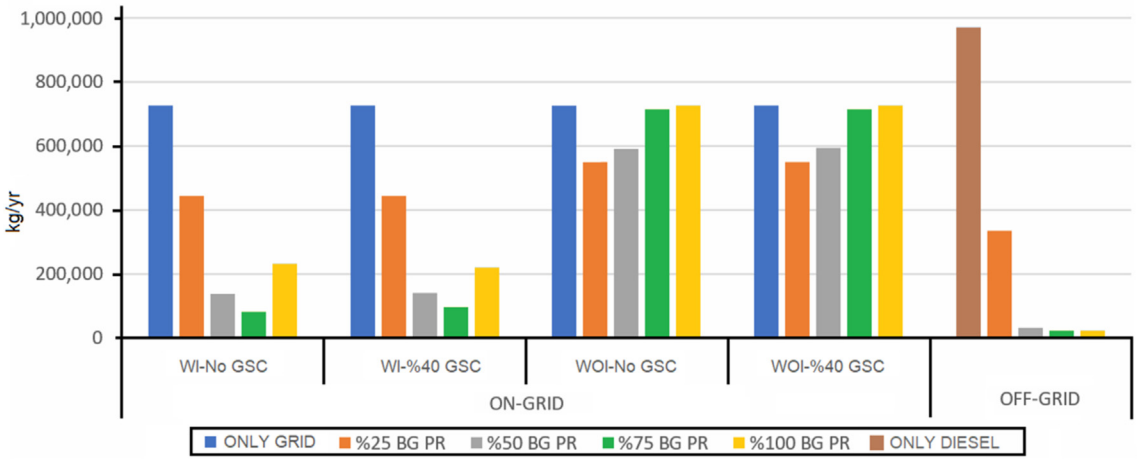


**Fig. 13.** $CO_2$ emissions.

emissions, helping to achieve the environmental targets. Fig. 14 shows the effects of CC variations of off-grid and on-grid HPS on PE, COE, IC, NPC, and RF. The CC decreases in parallel with the increase in the BG installed power for $2141 and below costs. CF was decreased at CC values above $2141 due to GSC. Therefore, COE did not reduce. COE of off-grid HPS scenario increases due to the increase in CC. The rising of CC increased the COE of on-grid HPS, resulting in a decrease in PE. For example, if CC is $1,495, 1.21 MWh

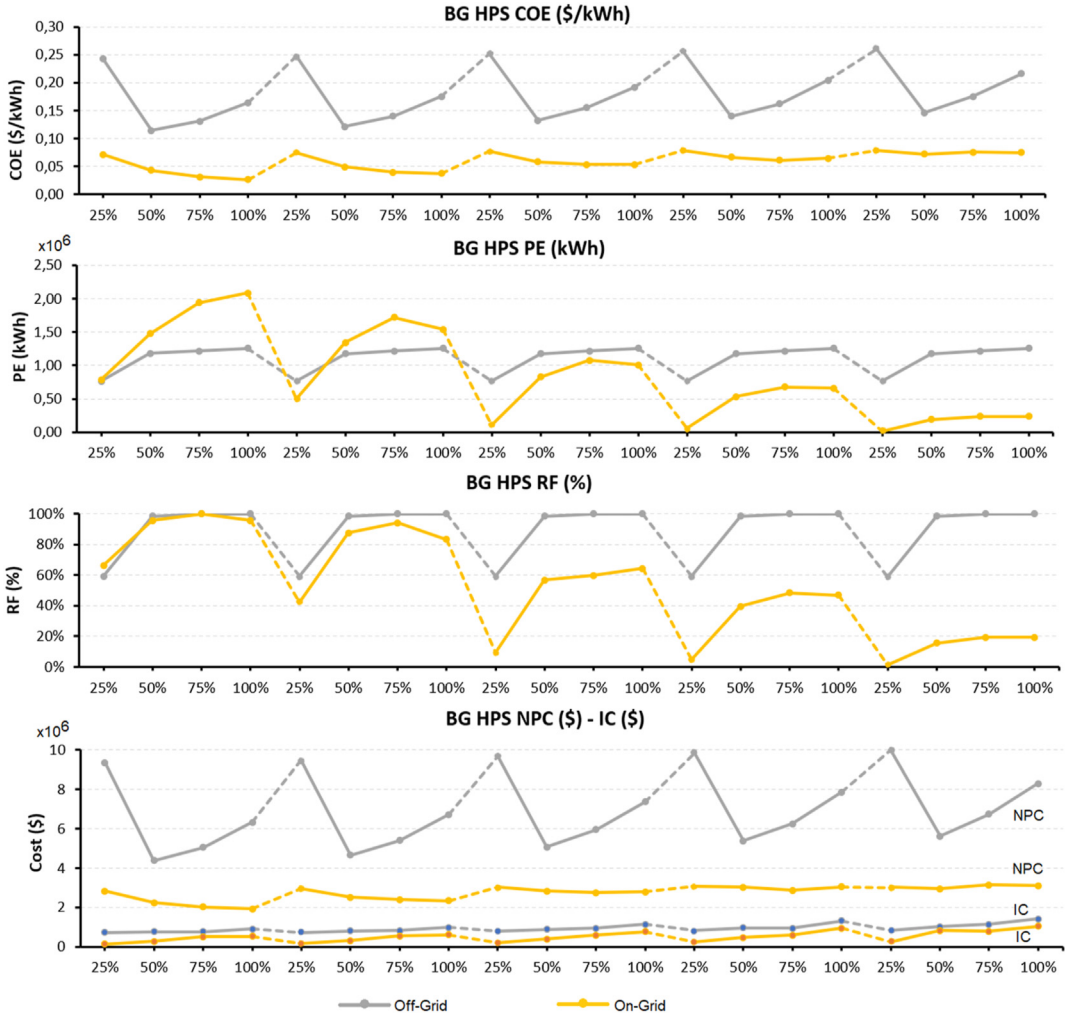


**Fig. 14.** Technical-economic variations according to CC.

PE was realized, but CC is $2,897, 0.23 MWh PE was realized due to increasing COE. The PE of the off-grid HPS scenarios took approximately the same values. CC remained below the COE with DG even though CC increased to its highest value of $2897. If CC increases by 20% to $2,141, then NPC's value increases by 9% compared to the case in off-grid HPS with 75% PR and CC at $1693. On the other hand, NPC increased by 13% for similar scenarios of on-grid HPS. The optimal RF was obtained in 50–75% PR of on-grid scenarios. Rising CC increased the COE, RF rates dropped to 19.2%, especially when CC was greater than $2897. If CC was greater than $1,693, RF was reduced by about 30%. Due to the decrease in PE, NPC was close or higher than the only grid scenario, thus eliminating the applicability of HPS.

### 3.4. Optimization Result-3 (hybrid HPS)

Table 6 shows the technical and economic results of on-grid HPS. The installed power is met with renewables in every option using PV, WT, and BG with different PRs. The increase in the PR of the on-grid BG causes the decrease in CFs due to GSC. Therefore, the DP period is prolonged, and the investment profitability decreases. Proper sizing of the PV-WT to be used is of great importance to increase energy continuity and reliability. Besides, the regional solar and wind potential and the system installation costs in $/kW can affect HPS components sizes. Table 5 shows that the best COE with 90 kW BG is in M1. It has been determined that PE is maximum in M3, where PV-WT powers are similar, and EE has the lowest value for M1-M4 scenarios. In addition, it has been observed that any of the PV or WT installed powers are high, increasing the EE and thus reducing the RF somewhat. The RF increased with the 180 kW BG in the on-grid M5-M8 scenarios. The IC and O&M costs of PV are less than WT. The availability of regional climatic conditions has provided the best NPC in M5, containing 180 kW of PV. As the PV-WT installed power in M5-M8 decreased, compared to M1-M4, EE approached zero. Increasing the share of WT in M5-M8 increased both COE and EE. On-grid BG with 75% PR (M10) showed that RF was highest and COE got the best. M10 with PV-WT supported BG with 75% PR decreased the COE obtained with BG with 100% PR in Table 4, increasing the RF ratio by approximately 10%, as shown in Fig. 11. On-grid biomass-based HPS optimization results show that the optimum scenario is formed in M10. HPS technical and economic parameters are improved if 100% PR BG is supported with accurate PV-WT. The analyzes of the scenarios in Fig. 15 are shown in Tables 5 and 6.

Table 6 shows the installed power variation of technical and economic effects on off-grid HPS containing both PV and WT with 100% PR. M5-500 kWh, which is with off-grid and BG with 50% PR, has realized optimal NPC. The RF was approximately 90% and above for 50–75% PR. EE is minimized in all off-grid scenarios with a 500 kWh battery. EE values increased and RF rates decreased by 20–35% in especially off-grid scenarios without battery. PE and COE increased nearly 15% and 12%, respectively, when comparing M9-500 kWh to M5-500 kWh.

## 4. Conclusions

Hybrid power systems can minimize energy deficit by integrating flexible generation capable renewable sources like biomass, especially in rural areas. With the development of the poultry farming industry in recent years, biomass energy generation is a promising alternative besides PV and WT. This study deals with optimizing energy storage integrated biomass-based HPS for the energy demand of a rural region containing poultry farms and minimizing the environmental effects of poultry farm wastes. Besides, overall technical-environmental-economic performances were evaluated off-grid and on-grid HPS with solar and wind energy. Energy storage integrated HPS has offered to economically sizing thanks to biomass energy generation. Solar PV integration

**Table 6**
The system performance of off-grid HPS RES with 100% PR.

| Case | BG (kW) | WT (kW) | PV (kW) | ESS (kWh) | COE ($/kWh) | NPC (M$) | IC (M$) | PE (MWh/yr) | Biomass (ton) | RF (%) | EE (kWh/yr) |
|---|---|---|---|---|---|---|---|---|---|---|---|
| **M1** | **90** | - | 270 | - | 0.405 | 15.5 | 0.73 | 465.1 | 2367 | 57.3 | 144,388 |
| | | | | 500 | 0.290 | 11.1 | 0.84 | 543.6 | 2756 | 73.6 | 13,338 |
| | | | | 1000 | 0.289 | 11.1 | 0.95 | 532.1 | 2697 | 73.7 | - |
| **M2** | | 50 | 220 | - | 0.397 | 15.2 | 0.84 | 454.2 | 2314 | 58.8 | 119,162 |
| | | | | 500 | 0.285 | 10.9 | 0.95 | 538.8 | 2734 | 74.6 | 4031 |
| | | | | 1000 | 0.287 | 11.0 | 1.06 | 531.2 | 2695 | 74.3 | 2.16 |
| **M3** | | 150 | 120 | - | 0.387 | 14.9 | 1.06 | 451.9 | 2306 | 61.0 | 98,716 |
| | | | | 500 | 0.286 | 11.0 | 1.17 | 526.6 | 2673 | 74.7 | 2513 |
| | | | | 1000 | 0.289 | 11.1 | 1.28 | 523.8 | 2659 | 74.6 | 131 |
| **M4** | | 250 | 20 | - | 0.383 | 14.7 | 1.27 | 473.5 | 2415 | 61.9 | 117,058 |
| | | | | 500 | 0.292 | 11.2 | 1.39 | 526.9 | 2670 | 74.3 | 13,573 |
| | | | | 1000 | 0.291 | 11.2 | 1.50 | 525.6 | 2663 | 74.8 | 3186 |
| **M5** | **180** | - | 180 | - | 0.217 | 8.33 | 0.79 | 938.4 | 4838 | 87.7 | 157,410 |
| | | | | 500 | 0.125 | 4.81 | 0.90 | 924.7 | 4732 | 98.0 | 3095 |
| | | | | 1000 | 0.131 | 5.05 | 1.01 | 917.1 | 4693 | 97.7 | 2.30 |
| **M6** | | 50 | 130 | - | 0.215 | 8.26 | 0.90 | 932.3 | 4812 | 88.4 | 146.673 |
| | | | | 500 | 0.129 | 4.97 | 1.01 | 916.0 | 4691 | 97.9 | 420 |
| | | | | 1000 | 0.134 | 5.17 | 1.12 | 913.3 | 4677 | 97.7 | 3.90 |
| **M7** | | 100 | 80 | - | 0.213 | 8.20 | 1.01 | 933.5 | 4820 | 89.1 | 143,353 |
| | | | | 500 | 0.134 | 5.16 | 1.12 | 908.2 | 4652 | 97.6 | 217 |
| | | | | 1000 | 0.139 | 5.32 | 1.23 | 907.0 | 4646 | 97.5 | 3.89 |
| **M8** | | 150 | 30 | - | 0.213 | 8.16 | 1.12 | 940.6 | 4854 | 89.5 | 148,781 |
| | | | | 500 | 0.137 | 5.27 | 1.23 | 903.1 | 4624 | 97.5 | 583 |
| | | | | 1000 | 0.142 | 5.44 | 1.34 | 901.4 | 4615 | 97.4 | 2.05 |
| **M9** | **270** | - | 90 | - | 0.163 | 6.25 | 0.85 | 1,315.1 | 6826 | 98.5 | 297,983 |
| | | | | 500 | 0.141 | 5.43 | 0.96 | 1,079.2 | 5583 | 100 | 999 |
| | | | | 1000 | 0.145 | 5.58 | 1.08 | 1,078.8 | 5580 | 100 | 0.361 |
| **M10** | | 50 | 40 | - | 0.164 | 6.31 | 0.96 | 1,310.0 | 6801 | 98.6 | 294,163 |
| | | | | 500 | 0.145 | 5.55 | 1.07 | 1,075.9 | 5568 | 100 | 250 |
| | | | | 1000 | 0.148 | 5.70 | 1.19 | 1,076.0 | 5569 | 100 | 0 |

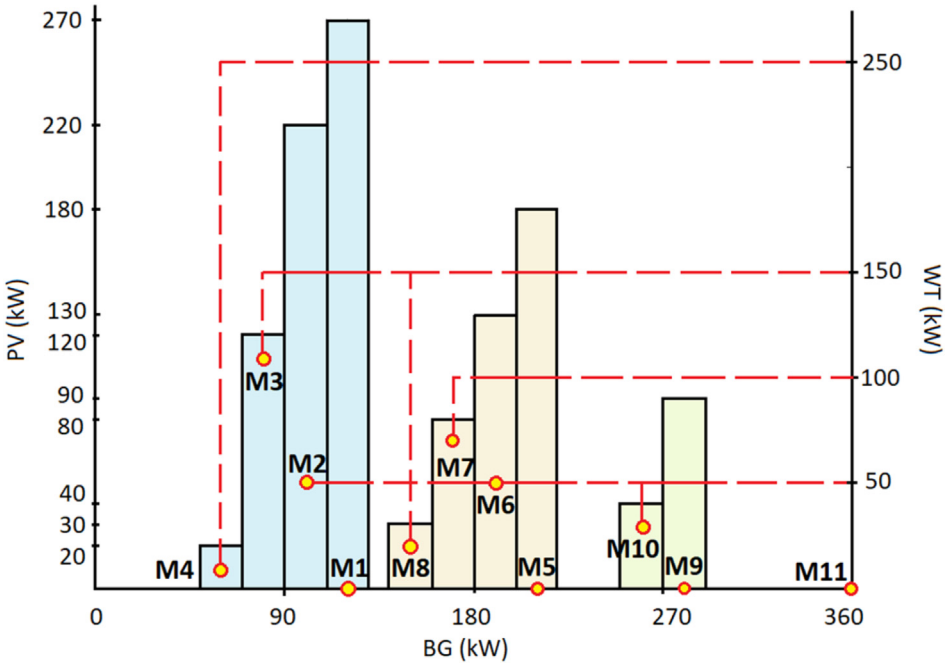


**Fig. 15.** HPS installed power modeling (RES with 100% PR).

into on-grid biomass-based HPS was reduced the NPV by approximately 12% and increased RF by 7% if PR is 100%. Moreover, the energy storage integration into off-grid biomass-based HPS increased RF approximately 10% and reduced excess energy by 16%. The result shows that the proposed biomass-based HPS may support decarbonization targets. Sensitivity analyses have revealed that the investment, raw material transportation, and O&M cost affect the on-grid or off-grid applicability of biomass-based HPS. Energy sales restrictions and incentives significantly affected the economic feasibility of pure biomass-based hybrid systems. Self-consumption was maximized without the biomass incentive, while the incentives led to selling an approximate 30% of generated energy to the grid. Furthermore, the energy exchange rate has been decreased to minimize grid dependency, resulting in better reliability. Results have shown that the incentives helped shorten the discount payback period to less than ten years, making HPS economically viable. In contrast, discount payback periods were close to project lifetimes in scenarios without incentive. Therefore, incentives significantly affect the economic feasibility of pure biomass-based hybrid systems. Thus, policymakers should support biomass and energy storage systems integrated hybrid renewable energy systems, especially for rural electrifications. The findings of the study can expanded to different industrial poultry farms with varying economic inputs and renewable resources.

## Funding

This research did not receive any specific grant from funding agencies in the public, commercial, or not-for-profit sectors.

## CRediT authorship contribution statement

**Alpaslan Demirci:** Conceptualization, Investigation, Resources, Methodology, Visualization, Software, Data curation, Writing – original draft, Writing – review & editing, Supervision. **Onur Akar:** Investigation, Resources, Writing – original draft. **Zafer Ozturk:** Methodology, Visualization, Investigation, Software, Data curation, Resources, Writing – original draft.

## Declaration of competing interest

The authors declare that they have no known competing financial interests or personal relationships that could have appeared to influence the work reported in this paper.

## References

[1] J. Ahmad, M. Imran, A. Khalid, W. Iqbal, S.R. Ashraf, M. Adnan, S.F. Ali, K.S. Khokhar, Techno economic analysis of a wind-photovoltaic-biomass hybrid renewable energy system for rural electrification: a case study of Kallar Kahar, Energy 148 (2018) 208–234, https://doi.org/10.1016/j.energy.2018.01.133.
[2] D. Jeong, J. Kim, D. Choi, E. Park, Social networking services as new venue for public perceptions of energy issues: the case of Paris agreement, Energy Strategy Rev. 39 (2022), 100758, https://doi.org/10.1016/j.esr.2021.100758.
[3] M.H. Jahangir, M. Montazeri, S.A. Mousavi, A. Kargarzadeh, Reducing carbon emissions of industrial large livestock farms using hybrid renewable energy systems, Renew. Energy 189 (2022) 52–65, https://doi.org/10.1016/j.renene.2022.02.022.
[4] G. Ferrari, P. Ai, A. Alengebawy, F. Marinello, A. Pezzuolo, An assessment of nitrogen loading and biogas production from Italian livestock: a multilevel and spatial analysis, J. Clean. Prod. 317 (2021), 128388, https://doi.org/10.1016/j.jclepro.2021.128388.
[5] J.L. Ramos-Suárez, A. Ritter, J. Mata González, A. Camacho Pérez, Biogas from animal manure: a sustainable energy opportunity in the Canary Islands, Renew. Sustain. Energy Rev. 104 (2019) 137–150, https://doi.org/10.1016/j.rser.2019.01.025.
[6] P. Abdeshahian, J.S. Lim, W.S. Ho, H. Hashim, C.T. Lee, Potential of biogas production from farm animal waste in Malaysia, Renew. Sustain. Energy Rev. 60 (2016) 714–723, https://doi.org/10.1016/j.rser.2016.01.117.
[7] G. Markou, Improved anaerobic digestion performance and biogas production from poultry litter after lowering its nitrogen content, Bioresour. Technol. 196 (2015) 726–730, https://doi.org/10.1016/j.biortech.2015.07.067.
[8] M. Caliskan, N.F. Tumen Ozdil, Potential of biogas and electricity production from animal waste in Turkey, BioEnergy Res. 14 (2021) 860–869, https://doi.org/10.1007/s12155-020-10193-w.
[9] J. Oláh, P. Lengyel, P. Balogh, M. Harangi-Rákos, J. Popp, The role of biofuels in food commodity prices volatility and land use, J. Compet. 9 (2017) 81–93, https://doi.org/10.7441/joc.2017.04.06.
[10] L. Hermann, R. Hermann, O.F. Schoumans, Report on Regulations Governing Anaerobic Digesters and Nutrient Recovery and Reuse in EU Member States, 2019, https://doi.org/10.18174/476673.
[11] S. Abanades, H. Abbaspour, A. Ahmadi, B. Das, M.A. Ehyaei, F. Esmaeilion, M. El

Haj Assad, T. Hajilounezhad, D.H. Jamali, A. Hmida, H.A. Ozgoli, S. Safari, M. AlShabi, E.H. Bani-Hani, A critical review of biogas production and usage with legislations framework across the globe, Int. J. Environ. Sci. Technol. 19 (2022) 3377–3400, https://doi.org/10.1007/s13762-021-03301-6.
[12] M. Gustafsson, S. Anderberg, Biogas policies and production development in Europe: a comparative analysis of eight countries, 0, Biofuels (2022) 1–14, https://doi.org/10.1080/17597269.2022.2034380.
[13] Luc Pelkmans, Implementation of Bioenergy in the IEA, 2021. https://www.ieabioenergy.com/wp-content/uploads/2021/11/CountriesReport2021_final.pdf.
[14] D. Saygin, O.B. Tör, M.E. Cebeci, S. Teimourzadeh, P. Godron, Increasing Turkey's power system flexibility for grid integration of 50% renewable energy share, Energy Strategy Rev. 34 (2021), https://doi.org/10.1016/j.esr.2021.100625.
[15] IRENA Renewable Cost Database, Renewable Power Generation Costs in 2020, 2020. https://www.irena.org/-/media/Files/IRENA/Agency/Publication/2018/Jan/IRENA_2017_Power_Costs_2018.pdf.
[16] M. Ozturk, N. Saba, V. Altay, R. Iqbal, K.R. Hakeem, M. Jawaid, F.H. Ibrahim, Biomass and bioenergy: an overview of the development potential in Turkey and Malaysia, Renew. Sustain. Energy Rev. 79 (2017) 1285–1302, https://doi.org/10.1016/j.rser.2017.05.111.
[17] A.K.S. Parihar, V. Sethi, R. Banerjee, Sizing of biomass based distributed hybrid power generation systems in India, Renew. Energy 134 (2019) 1400–1422, https://doi.org/10.1016/j.renene.2018.09.002.
[18] N. Bhatnagar, D. Ryan, R. Murphy, A.M. Enright, A comprehensive review of green policy, anaerobic digestion of animal manure and chicken litter feedstock potential – global and Irish perspective, Renew. Sustain. Energy Rev. 154 (2022), 111884, https://doi.org/10.1016/j.rser.2021.111884.
[19] M.M. Ibrahim, N.H. Mostafa, A.H. Osman, A. Hesham, Performance analysis of a stand-alone hybrid energy system for desalination unit in Egypt, Energy Convers. Manag. 215 (2020), 112941, https://doi.org/10.1016/j.enconman.2020.112941.
[20] C. Miao, K. Teng, Y. Wang, L. Jiang, Technoeconomic analysis on a hybrid power system for the UK household using renewable energy: a case study, Energies 13 (2020) 3231, https://doi.org/10.3390/en13123231.
[21] A. Bhatt, M.P. Sharma, R.P. Saini, Feasibility and sensitivity analysis of an off-grid micro hydro–photovoltaic–biomass and biogas–diesel–battery hybrid energy system for a remote area in Uttarakhand state, India, Renew. Sustain. Energy Rev. 61 (2016) 53–69, https://doi.org/10.1016/j.rser.2016.03.030.
[22] W. Uddin, B. Khan, N. Shaukat, M. Majid, G. Mujtaba, A. Mehmood, S.M. Ali, U. Younas, M. Anwar, A.M. Almeshal, Biogas potential for electric power generation in Pakistan: a survey, Renew. Sustain. Energy Rev. 54 (2016) 25–33, https://doi.org/10.1016/j.rser.2015.09.083.
[23] R. Rajbongshi, D. Borgohain, S. Mahapatra, Optimization of PV-biomass-diesel and grid base hybrid energy systems for rural electrification by using HOMER, Energy 126 (2017) 461–474, https://doi.org/10.1016/j.energy.2017.03.056.
[24] K.M. Kotb, M.R. Elkadeem, M.F. Elmorshedy, A. Dán, Coordinated power management and optimized techno-enviro-economic design of an autonomous hybrid renewable microgrid: a case study in Egypt, Energy Convers. Manag. 221 (2020), 113185, https://doi.org/10.1016/j.enconman.2020.113185.
[25] C. Mokhtara, B. Negrou, A. Bouferrouk, Y. Yao, N. Settou, M. Ramadan, Integrated supply–demand energy management for optimal design of off-grid hybrid renewable energy systems for residential electrification in arid climates, Energy Convers. Manag. 221 (2020), 113192, https://doi.org/10.1016/j.enconman.2020.113192.
[26] C. Brandoni, B. Bošnjaković, HOMER analysis of the water and renewable energy nexus for water-stressed urban areas in Sub-Saharan Africa, J. Clean. Prod. 155 (2017) 105–118, https://doi.org/10.1016/j.jclepro.2016.07.114.
[27] M. Singh, P. Balachandra, Microhybrid electricity system for energy access, livelihoods, and empowerment, Proc. IEEE 107 (2019) 1995–2007, https://doi.org/10.1109/JPROC.2019.2910834.
[28] M. Arshad, I. Bano, N. Khan, M.I. Shahzad, M. Younus, M. Abbas, M. Iqbal, Electricity generation from biogas of poultry waste: an assessment of potential and feasibility in Pakistan, Renew. Sustain. Energy Rev. 81 (2018) 1241–1246, https://doi.org/10.1016/j.rser.2017.09.007.
[29] G. Ali, M.K. Bashir, H. Ali, M.H. Bashir, Utilization of rice husk and poultry wastes for renewable energy potential in Pakistan: an economic perspective, Renew. Sustain. Energy Rev. 61 (2016) 25–29, https://doi.org/10.1016/j.rser.2016.03.014.
[30] M.R. Saravanan, A. Pasupathy, Incorporation of phase change material (PCM) in poultry Hatchery for thermal management & energy conversion schemes of slaughterhouse waste in Broiler farms for energy conservation - a case study, in: 2016 Int. Conf. Energy Effic. Technol. Sustain, IEEE, 2016, pp. 291–299, https://doi.org/10.1109/ICEETS.2016.7583768.
[31] J. Li, P. Liu, Z. Li, Optimal design and techno-economic analysis of a solar-wind-biomass off-grid hybrid power system for remote rural electrification: a case study of west China, Energy 208 (2020), 118387, https://doi.org/10.1016/j.energy.2020.118387.
[32] S. Singh, M. Singh, S.C. Kaushik, Feasibility study of an islanded microgrid in rural area consisting of PV, wind, biomass and battery energy storage system, Energy Convers. Manag. 128 (2016) 178–190, https://doi.org/10.1016/j.enconman.2016.09.046.
[33] J. Singh, B. Panesar, S. Sharma, Energy potential through agricultural biomass using geographical information system—a case study of Punjab, Biomass Bioenergy 32 (2007) 301–307, https://doi.org/10.1016/j.biombioe.2007.10.003.
[34] S. Singh, S.C. Kaushik, Optimal sizing of grid integrated hybrid PV-biomass energy system using artificial bee colony algorithm, IET Renew. Power Gener. 10 (2016) 642–650, https://doi.org/10.1049/iet-rpg.2015.0298.
[35] D.M. Alotaibi, M. Akrami, M. Dibaj, A.A. Javadi, Smart energy solution for an optimised sustainable hospital in the green city of NEOM, Sustain. Energy Technol. Assessments 35 (2019) 32–40, https://doi.org/10.1016/j.seta.2019.05.017.
[36] P. Balamurugan, S. Ashok, T.L. Jose, Optimal operation of biomass/wind/PV hybrid energy system for rural areas, Int. J. Green Energy 6 (2009) 104–116, https://doi.org/10.1080/15435070802701892.
[37] M.W. Rahman, M.S. Hossain, A. Aziz, F.M. Mohammedy, Prospect of decentralized hybrid power generation in Bangladesh using biomass, solar PV & wind, in: 2014 3rd Int. Conf. Dev. Renew. Energy Technol, IEEE, 2014, pp. 1–6, https://doi.org/10.1109/ICDRET.2014.6861690.
[38] W.S. Ho, H. Hashim, J.S. Lim, Integrated biomass and solar town concept for a smart eco-village in Iskandar Malaysia (IM), Renew. Energy 69 (2014) 190–201, https://doi.org/10.1016/j.renene.2014.02.053.
[39] A. Heydari, A. Askarzadeh, Optimization of a biomass-based photovoltaic power plant for an off-grid application subject to loss of power supply probability concept, Appl. Energy 165 (2016) 601–611, https://doi.org/10.1016/j.apenergy.2015.12.095.
[40] T. Sarkar, A. Bhattacharjee, H. Samanta, K. Bhattacharya, H. Saha, Optimal design and implementation of solar PV-wind-biogas-VRFB storage integrated smart hybrid microgrid for ensuring zero loss of power supply probability, Energy Convers. Manag. 191 (2019) 102–118, https://doi.org/10.1016/j.enconman.2019.04.025.
[41] F. Baghdadi, K. Mohammedi, S. Diaf, O. Behar, Feasibility study and energy conversion analysis of stand-alone hybrid renewable energy system, Energy Convers. Manag. 105 (2015) 471–479, https://doi.org/10.1016/j.enconman.2015.07.051.
[42] N. Ramchandran, R. Pai, A.K.S. Parihar, Feasibility assessment of Anchor-Business-Community model for off-grid rural electrification in India, Renew. Energy 97 (2016) 197–209, https://doi.org/10.1016/j.renene.2016.05.036.
[43] M.S. Islam, R. Akhter, M.A. Rahman, A thorough investigation on hybrid application of biomass gasifier and PV resources to meet energy needs for a northern rural off-grid region of Bangladesh: a potential solution to replicate in rural off-grid areas or not? Energy 145 (2018) 338–355, https://doi.org/10.1016/j.energy.2017.12.125.
[44] S. Bhattacharjee, A. Dey, Techno-economic performance evaluation of grid integrated PV-biomass hybrid power generation for rice mill, Sustain. Energy Technol. Assessments 7 (2014) 6–16, https://doi.org/10.1016/j.seta.2014.02.005.
[45] M.S. Hossain, A. Jahid, K.Z. Islam, M.F. Rahman, Solar PV and biomass resources-based sustainable energy supply for off-grid cellular base stations, IEEE Access 8 (2020) 53817–53840, https://doi.org/10.1109/ACCESS.2020.2978121.
[46] M.H. Jahangir, S. Fakouriyan, M.A. Vaziri Rad, H. Dehghan, Feasibility study of on/off grid large-scale PV/WT/WEC hybrid energy system in coastal cities: a case-based research, Renew. Energy 162 (2020) 2075–2095, https://doi.org/10.1016/j.renene.2020.09.131.
[47] A. Baruah, M. Basu, D. Amuley, Modeling of an autonomous hybrid renewable energy system for electrification of a township: a case study for Sikkim, India, Renew. Sustain. Energy Rev. 135 (2021), 110158, https://doi.org/10.1016/j.rser.2020.110158.
[48] V. Suresh, M. M, R. Kiranmayi, Modelling and optimization of an off-grid hybrid renewable energy system for electrification in a rural areas, Energy Rep. 6 (2020) 594–604, https://doi.org/10.1016/j.egyr.2020.01.013.
[49] S.A. Mousavi, R.A. Zarchi, F.R. Astaraei, R. Ghasempour, F.M. Khaninezhad, Decision-making between renewable energy configurations and grid extension to simultaneously supply electrical power and fresh water in remote villages for five different climate zones, J. Clean. Prod. 279 (2021), 123617, https://doi.org/10.1016/j.jclepro.2020.123617.
[50] C.L. Chambon, T. Karia, P. Sandwell, J.P. Hallett, Techno-economic assessment of biomass gasification-based mini-grids for productive energy applications: the case of rural India, Renew. Energy 154 (2020) 432–444, https://doi.org/10.1016/j.renene.2020.03.002.
[51] H. Garrido, V. Vendeirinho, M.C. Brito, Feasibility of KUDURA hybrid generation system in Mozambique: sensitivity study of the small-scale PV-biomass and PV-diesel power generation hybrid system, Renew. Energy 92 (2016) 47–57, https://doi.org/10.1016/j.renene.2016.01.085.
[52] M.S. Adaramola, M. Agelin-Chaab, S.S. Paul, Analysis of hybrid energy systems for application in southern Ghana, Energy Convers. Manag. 88 (2014) 284–295, https://doi.org/10.1016/j.enconman.2014.08.029.
[53] M.S. Adaramola, M. Agelin-Chaab, S.S. Paul, Analysis of hybrid energy systems for application in southern Ghana, Energy Convers. Manag. 88 (2014) 284–295, https://doi.org/10.1016/j.enconman.2014.08.029.
[54] H. Rezk, M. Al-Dhaifallah, Y.B. Hassan, H.A. Ziedan, Optimization and energy management of hybrid photovoltaic-diesel-battery system to pump and desalinate water at isolated regions, IEEE Access 8 (2020) 102512–102529, https://doi.org/10.1109/ACCESS.2020.2998720.
[55] M.S. Javed, T. Ma, J. Jurasz, F.A. Canales, S. Lin, S. Ahmed, Y. Zhang, Economic analysis and optimization of a renewable energy based power supply system with different energy storages for a remote island, Renew. Energy 164 (2021)

1376–1394, https://doi.org/10.1016/j.renene.2020.10.063.
[56] G. Kaur, N.K. Sharma, J. Kaur, M. Bajaj, H.M. Zawbaa, R.A. Turky, S. Kamel, Prospects of biogas and evaluation of unseen livestock based resource potential as distributed generation in India, Ain Shams Eng. J. (2021), 101657, https://doi.org/10.1016/j.asej.2021.101657.
[57] A.O. Avcioğlu, U. Türker, Status and potential of biogas energy from animal wastes in Turkey, Renew. Sustain. Energy Rev. 16 (2012) 1557–1561, https://doi.org/10.1016/j.rser.2011.11.006.
[58] Y. Kirim, H. Sadikoglu, M. Melikoglu, Technical and economic analysis of biogas and solar photovoltaic (PV) hybrid renewable energy system for dairy cattle barns, Renew. Energy 188 (2022) 873–889, https://doi.org/10.1016/j.renene.2022.02.082.
[59] M. Mudasser, E.K. Yiridoe, K. Corscadden, Cost-benefit analysis of grid-connected wind–biogas hybrid energy production, by turbine capacity and site, Renew. Energy 80 (2015) 573–582, https://doi.org/10.1016/j.renene.2015.02.055.
[60] F. Al-Turjman, Z. Qadir, M. Abujubbeh, C. Batunlu, Feasibility analysis of solar photovoltaic-wind hybrid energy system for household applications, Comput, Electr. Eng. 86 (2020), 106743, https://doi.org/10.1016/j.compeleceng.2020.106743.
[61] L. Olatomiwa, S. Mekhilef, A.S.N. Huda, K. Sanusi, Techno-economic analysis of hybrid PV–diesel–battery and PV–wind–diesel–battery power systems for mobile BTS: the way forward for rural development, Energy Sci. Eng. 3 (2015) 271–285, https://doi.org/10.1002/ese3.71.
[62] C. Li, Y. Zheng, Z. Li, L. Zhang, L. Zhang, Y. Shan, Q. Tang, Techno-economic and environmental evaluation of grid-connected and off-grid hybrid intermittent power generation systems: a case study of a mild humid subtropical climate zone in China, Energy 230 (2021), 120728, https://doi.org/10.1016/j.energy.2021.120728.
[63] Y.E. Unutmaz, A. Demirci, S.M. Tercan, R. Yumurtaci, Electrical energy demand forecasting using artificial neural network, in: 2021 3rd Int. Congr. Human-Computer Interact. Optim. Robot. Appl, IEEE, 2021, pp. 1–6, https://doi.org/10.1109/HORA52670.2021.9461186.
[64] Z. Ozturk, A. Demirci, S. Tosun, A. Ozturk, Technic and economic effects of changes in the location of industrial facilities in industrializing regions on power systems, in: 2021 13th Int. Conf. Electr. Electron. Eng, IEEE, 2021, pp. 11–17, https://doi.org/10.23919/ELECO54474.2021.9677827.
[65] S.M. Tercan, A. Demirci, E. Gokalp, U. Cali, Maximizing self-consumption rates and power quality towards two-stage evaluation for solar energy and shared energy storage empowered microgrids, J. Energy Storage 51 (2022), 104561, https://doi.org/10.1016/j.est.2022.104561.